https://doi.org/10.2352/EI.2026.38.3.MOBMU-347

Automation of a Stereotaxic Device through Neuroanatomical Atlas Integrated Motion Control: A Modular Retrofit Approach for Precision Neuroscience Applications

Johnssi Manjunath[1], Lukasz Rojek[1], York Winter[2]; [1]SRH University, Berlin School of Technology and Architecture, Sonnenallee 221, D-12587 Berlin, Germany; [2]Humboldt Universität, Berlin, Germany

Abstract

Stereotaxic neurosurgery in small-animal neuroscience remains largely manual and operator-dependent, introducing variability that compromises experimental reproducibility [1,2]. This paper presents a modular retrofit system that motorises a conventional rodent stereotaxic frame and integrates it with Pinpoint [9] for neuroanatomic positioning via a custom Ephys Link binding [10], enabling direct software-to-hardware coordinate translation from neuroanatomical atlas-based planning to physical needle insertion. The system uses NEMA 17 stepper motors with a 14:1 planetary gearbox, a Duet 3 Mini 5+ motion controller [8] originally developed for open-source 3D printing and here adapted for neuroscience through developer collaboration, and RepRapFirmware configured in CNC mode. A custom firmware parameter (M203 I0.1) unlocks a minimum feed rate of 0.1 mm/min for tissue-safe brain insertion. The microinjection axis is fully automated for suction and retraction. A custom housing provides structural rigidity, vibration damping, and cable management without modifying the original frame. The system achieves positional accuracy beyond 0.1mm, with a nominal microstep increment of 0.09µm, validated using phantoms and ex vivo specimens.

Keywords: *stereotaxic surgery, laboratory automation, motion control, microinjection, software–hardware integration, Duet3D, Pinpoint, open-source, reproducibility*

1. Introduction

Stereotaxic surgery is the cornerstone technique in experimental neuroscience for precisely targeting brain structures in small rodents through microinjections, viral vector delivery, and electrode placement. The technique demands sub-millimetre positioning accuracy; a deviation of even 100 µm can engage an entirely different functional structure [1]. Despite this stringent requirement, the procedure often remains manual and reliant on operator skill, concentration, and sustained fine motor control.

Manual stereotaxic workflows introduce variability through inconsistent injection speeds and operator fatigue across repeated procedures. Targeting failures imposes additional surgeries that should be avoided.

Fully robotic stereotaxic platforms exist but are closed-source, proprietary, and expensive, placing them beyond the reach of many research groups [6]. When moving to automation, these systems require the complete replacement of existing infrastructure, which is impractical given the large installed base of manual frames in neuroscience laboratories worldwide.

Prior open-source efforts have demonstrated that existing frames can be retrofitted at modest cost [7], enabling reproducible tool paths and reducing manual micrometric adjustment. However, these implementations relied on PC-tethered serial-port CNC controllers and manually authored G-code scripts, with no real-time integration with neuroanatomical atlas-based planning software [7]. Coordinate transcription from planning tool to motor command remained a manual, error-prone step. The present work addresses this gap by combining a modern networked motion controller, originally developed for open-source 3D printing and domain-adapted through developer collaboration, with direct middleware binding between a neuroanatomical 3D planning environment and physical hardware execution.

Coffey et al. [7] demonstrated that an existing stereotaxic frame can be motorised with CNC components. More recently, Ly et al. [11] presented a robotic targeting approach that dynamically aligns the subject based on a 3D-mapped profile of the skull's surface, and Han et al. [12] demonstrated robot-assisted microinjection for cell transplantation. The present work combines the retrofit philosophy [7] with a 32-bit networked motion controller, firmware-level ultra-low speed adaptation, and middleware-level neuroanatomical planning integration, completing the pipeline from neuroanatomical atlas-based coordinate definition to physical needle insertion.

2. System Design and Architecture

2.1 Design Philosophy

The system is built around three core principles: (1) modularity, all components are independently replaceable; (2) compatibility, the original frame geometry and manual override capability are fully preserved [7]; and (3) openness, all hardware, firmware, and software are open-source or openly documented [6, 7, 9]. A human-in-the-loop paradigm is maintained: the system automates tasks where machines are demonstrably superior, sustained low-speed motion, while leaving anatomical judgment to the researcher.

2.2 Base System and Rationale for Retrofitting

The base platform is a standard manual rodent stereotaxic frame. This work adopts the retrofit philosophy of Coffey et al. [7]: motorising an existing frame rather than constructing a new instrument. Most neuroscience laboratories already possess a stereotaxic frame, making retrofit considerably more practical than full replacement. Using a frame with proven mechanical geometry avoids introducing new anatomical alignment errors. The frame used here provided ±12.5 mm travel range on each translational axis (AP: Anterior-Posterior, ML: Medial-Lateral, DV: Dorsal-Ventral), sufficient for standard rodent stereotaxic targeting. Prior to motorisation, attachment points were identified that engage existing micrometre mechanisms without modifying frame geometry.

2.3 Actuation: X, Y, Z Axes

Stereotaxic actuation requirements are stringent: a positional accuracy of better than 0.1 mm and sustained slow motion at 0.1 mm/min when travelling inside live brain tissue to minimise damage [5]. Following iterative evaluation, NEMA 17 stepper motors with a 14:1 planetary gearbox were selected for the X, Y, and Z axes (AP, ML, DV). The gearbox multiplies effective resolution and torque, providing immunity from direct microstepping irregularities at ultra-low speeds. Motors were coupled to existing micrometre inputs via rigid shaft couplers with careful coaxial alignment.

2.4 Actuation: Microinjection Mechanism (U Axis)

The microinjection mechanism posed distinct challenges. Direct motor coupling is not possible, as it would induce unintended rotation of the motor body, thereby compromising actuation precision. To keep the motor rotationally fixed while allowing it to follow the injector's vertical travel, the rotational constraint was decoupled from translational freedom using a custom 3D-printed mechanism consisting of a hollow sleeve fixed to a reference rod and a cylindrical extension on the motor housing that slides within it. This arrangement supports both fluid suction and retraction with full proportional control. Following the evaluation of alternatives, a NEMA 8 rotary stepper motor was selected [8]. Unlike the X, Y, and Z axes, the NEMA 8 motor driving the injector axis does not incorporate a gearbox, and its motion is defined directly by the injector's mechanical transmission.

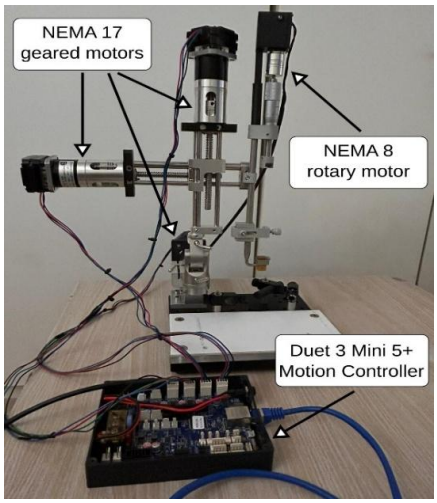

Fig. 1. *NEMA 17 geared motor (left) coupled to translational axis micrometre; NEMA 8 rotary motor (top right, coupled to injector) with 3D-printed rotational constraint mechanism for the microinjection (U) axis.*

2.5 Custom Mechanical Housing

System-level mechanical design (structural rigidity, vibration damping, cable management, electrical safety) is essential for reliable long-duration ultra-low-speed operation and is frequently underaddressed in open-source implementations. A custom housing fabricated via additive manufacturing addresses all these aspects. It provides structural rigidity against motor reaction loads, electrical isolation of live components, and cable routing, preventing interference with instrument travel. The housing mounts externally without modifying the original frame, preserving backward compatibility with manual operation.

2.6 Motion Controller, Firmware, and Domain Adaptation

The Duet 3 Mini 5+ is a 32-bit ARM-based motion controller from the open-source 3D printing community [8], featuring integrated TMC2209 stepper drivers, Ethernet/WiFi connectivity, and RepRapFirmware — a mature, actively maintained firmware ecosystem configurable entirely via G-code files, here repurposed for neuroscience. The system is configured in CNC mode (M453) with Cartesian kinematics, and four axes are defined: X (AP), Y (ML), Z (DV), and U (injector) [8].

A critical limitation was identified: RepRapFirmware's default minimum feed rate is designed for 3D printing speeds, far exceeding the 0.1 mm/min required for tissue-safe brain insertion. This was resolved through direct engagement with the RepRapFirmware development team, who extended the firmware to support the M203 I{0.1} parameter, setting a minimum feed rate of 0.1 mm/min as a single firmware line [8]. This exemplifies how a 3D printing platform, through open-source community collaboration, can be domain-adapted to meet precise biomedical requirements, an adaptation that is impossible in closed, proprietary systems [6].

Axis calibration was initialized from nominal drivetrain specifications and then refined by empirical calibration against measured travel. For the X, Y, and Z axes, the nominal configuration comprised a 200 steps/revolution motor, 16× microstepping, a nominal 14:1 planetary gearbox, and the frame's existing double-start micrometre screw with 2.0 mm pitch and 4.0 mm lead per revolution. These nominal parameters predict 11,200 steps/mm. Empirical calibration against measured axis displacement yielded an effective value of 10,926.8 steps/mm, which was used for motion control. Because the individual contributions of screw lead, gearbox ratio, and other drivetrain tolerances were not independently characterized, the 2.5% deviation from the nominal prediction is reported as an overall system calibration factor rather than attributed to a single mechanical component. The injector (U) axis is calibrated separately: with 16× microstepping and a transmission equivalent to 2 rotations/mm, it yields 6400 steps/mm. The governing calibration relationship is:

Steps/mm = (Steps/revolution × Microsteps × Gear ratio) / Lead (mm/revolution)

Calibration was performed by measuring linear displacement over multiple commanded movements to minimise measurement uncertainty. Additional motion parameters are configured at the firmware level: maximum feed rates (M203), acceleration (M201), and instantaneous speed-change limit / jerk parameter (M566 = 0 for all axes) to ensure smooth, controlled motion at ultra-low speeds. All parameters are version-controlled in firmware configuration files, supporting full methodological transparency and independent replication [8].

2.7 Software Integration: Pinpoint and Ephys Link

To bridge the gap between neuroanatomical atlas-based planning and physical execution, unaddressed in prior open-source work [7], the system integrates with Pinpoint [9], an open-source 3D

neuroanatomic stereotaxic planning environment that supports multi-probe trajectory definition based on the Paxinos & Franklin mouse brain atlas [14]. Pinpoint communicates with hardware via Ephys Link [10], an open-source middleware that uses HTTP server and Socket.IO for communication, providing a standardised API between planning software and physical manipulators.

No Duet-compatible binding existed in Ephys Link. A Duet-specific Python binding was developed by extending the *BaseBinding* class and registered under the CLI name "Duet". The binding exposes a single manipulator identified as "Duet", which appears in Pinpoint as "Manipulator Duet" following the frontend's naming convention. On initialisation, G92 X0 Y0 Z0 defines the current physical position as the coordinate origin. Pinpoint's stereotaxic Vector4 is remapped to Duet machine axes: *.y* (AP) → X; *.z* (ML) → Y; *.x* (DV) → Z. G-code commands are dispatched via HTTP GET to the Duet's */rr_gcode* endpoint at local IP address [8,10].

Two distinct motion modes enforce speed constraints. In *set_position* (lateral repositioning above the brain), a minimum of 30 mm/min is enforced for efficient repositioning. Critically, Z is commanded before XY — a safety design ensuring the probe is raised before any lateral movement, preventing tissue damage from sideways displacement while the probe is partially inserted. In *set_depth* (insertion into brain tissue), commands are issued in relative mode (G91→G1→G90) with sign inversion (Pinpoint +depth = down; Duet −Z = down), and the firmware-unlocked 0.1 mm/min minimum applies. Emergency stop is available via M0.

Table 1. Axis coordinate mapping and speed modes: Pinpoint → Duet controller.

Pinpoint	Duet Axis	Function
.y	X	AP
.z	Y	ML
.x	Z	DV (position)
.w	Z Δ (rel.)	Depth (brain)

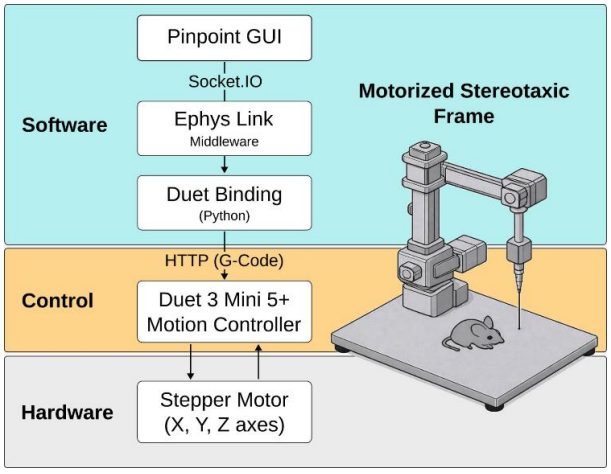

Fig. 2. *Pinpoint 3D neuroanatomical planning interface with the Duet-controlled stereotaxic manipulator and stepper motors registered via Ephys Link.*

3. Results and Validation

3.1 Mechanical Assembly and Baseline Functionality

Following motorisation, manual inspection confirmed that no visible frame deformation was observed. All three axes (X, Y, and Z) demonstrated smooth, bidirectional motion across the ±12.5 mm travel range with no observable backlash during directional reversals and no drift under static holding.

3.2 Positional Accuracy

Commanded displacements of 0.1, 1, and 10 mm were benchmarked against mechanical reference markers across the X, Y, and Z axes. Agreement was confirmed at a positioning accuracy of 0.1 mm, meeting the sub-millimetre accuracy standard for rodent stereotaxic targeting [1]. No cumulative drift was observed during repeated bidirectional sequences, and return-to-origin tests confirmed exact reproduction of initial reference coordinates.

3.3 Ultra-Low Speed Motion: 0.1 mm/min Inside Brain Tissue

The primary firmware contribution, minimum feed rate of 0.1 mm/min via M203 I{0.1} [8], was validated under sustained operation on bench and ex vivo specimens. Motion at 0.1 mm/min proceeded without stalling, oscillation, or vibration. Smooth holding-to-motion transitions were observed with no abrupt positional jumps. The enforced separation between 30 mm/min repositioning above the brain and 0.1 mm/min insertion into tissue was confirmed through repeated Pinpoint-commanded trajectories [5].

3.4 System Calibration and Axis Validation

Machine zero was established via G92 X0 Y0 Z0 on binding initialisation. Biological depth zero was set at dura surface contact, synchronising the depth coordinate to 0 mm and referencing all insertion commands to the anatomically relevant surface. Axis direction verification confirmed concordance with stereotaxic convention. The sign inversion in *set_depth* (Pinpoint +depth → Duet −Z) was validated through commanded depth sequences. Multi-axis tests confirmed correct directionality and absence of cross-axis interference.

3.5 Microinjection Actuation

The NEMA 8 motor with the rotational constraint demonstrated smooth, proportional plunger motion across multiple test cycles. Both fluid suction and retraction were executed without binding, torsional stress, or mechanical interference across the full 0–150 mm U-axis travel range.

3.6 Software Integration Validation

End-to-end integration was validated through Pinpoint-commanded trajectories. The binding registered correctly as "Manipulator Duet" [9,10]. Single-axis, multi-axis, and depth-specific movements produced correct physical motion. The Z-before-XY safety sequence was confirmed to correctly retract the probe before lateral repositioning. Depth insertion at 0.1 mm/min executed correctly regardless of the higher speeds requested by the planning software. The pipeline remained stable across repeated command sequences.

3.7 System Reproducibility

Motion characteristics were consistent across power cycles and sessions. All parameters, steps/mm (M92), feed rates (M203), acceleration (M201), jerk parameter (M566), and motor current (M906, M917), are defined in version-controlled firmware configuration files [8], enabling complete reproducibility from documented configuration without implicit knowledge or undocumented tuning.

4. Discussion

4.1 Interpretation of Results

The findings demonstrate that a conventional manual stereotaxic frame can be successfully retrofitted to achieve beyond 0.1 mm positional accuracy [1] and 0.1 mm/min tissue-safe insertion speed [5], with performance comparable to commercial robotic platforms [11,12], using open-source components. The critical enabler is the firmware-level minimum speed adaptation (M203 I{0.1}): without this, the Duet, designed for 3D printing speeds, could not sustain the ultra-low feed rates required for brain insertion. This corresponds to a nominal microstep increment of 0.0915 µm; experimentally, positional agreement was confirmed at 0.1 mm positioning accuracy. Direct neuroanatomical planning-to-hardware integration via Ephys Link eliminates manual brain coordinate transcription, removing a persistent source of operator-dependent variability [2,3].

4.2 Comparison with Existing Approaches

The present system builds directly on the retrofit concept of Coffey et al. [7], who demonstrated that a functional CNC stereotaxic instrument can be built from an existing frame using a TB6560 stepper driver board connected via DB25 parallel port to a PC running Mach3 CNC software, with surgery coordinates programmed through manually authored g-code scripts [7]. This established the viability of open-source stereotaxic retrofitting but left neuroanatomical coordinate transcription as a fully manual step, with no integration with atlas-based planning tools and no means of enforcing ultra-low insertion speeds programmatically.

The present work advances this foundation in three critical dimensions. First, the controller: the Duet 3 Mini 5+, a 32-bit networked motion controller from the 3D printing community, dispatches G-code over HTTP rather than requiring a tethered PC serial connection. The 14:1 planetary gearbox, combined with the TMC2209 drivers running 16× microstepping, yields 10,926.8 steps/mm with a nominal linear increment of 0.09 µm per microstep, far exceeding the half-step resolution of Coffey's TB6560 driver board. Critically, the firmware was domain-adapted through direct developer collaboration to support M203 I{0.1}, unlocking 0.1 mm/min as the minimum feed rate, a capability absent in 3D printing use cases and impossible to achieve in proprietary closed systems [6]. Second, software integration: the custom Ephys Link binding connects Pinpoint's neuroanatomical atlas-based planning directly to hardware [9,10], eliminating manual transcription entirely. Third, safety-aware motion sequencing: the Z-before-XY retraction order and mode-differentiated speeds (30 mm/min above the brain; 0.1 mm/min inside tissue) provide procedural safeguards not achievable in script-based G-code approaches.

This case also illustrates a broader principle: open-source hardware ecosystems developed for one domain, here, consumer 3D printing, can be systematically adapted to meet precision biomedical requirements through transparent community engagement [8]. This contrasts sharply with proprietary systems [6], where such domain-specific adaptations are impossible without vendor involvement.

4.3 Limitations

Validation is restricted to mechanical performance, motion characterisation, and software integration using phantoms and ex vivo specimens. No in vivo biological experiments were conducted, limiting the evaluation of tissue integrity or targeting success under realistic biological conditions.

Position tracking is open-loop: the binding maintains an internal state vector updated after each command, without encoder feedback from the physical axes. Any undetected mechanical slip would introduce an untracked error. Additionally, as Coffey et al. [7] noted, individual anatomical variation in skull morphology, differences in bregma-lambda distance, skull curvature, and thickness [14], contributes residual biological error that mechanical accuracy alone cannot correct.

4.4 Future Work

Three directions are prioritised: (1) in vivo validation in an animal facility; (2) closed-loop position verification to address open-loop tracking and detect mechanical slip in real time; and (3) automated cranial landmark detection, using convolutional neural networks to identify bregma and lambda in intraoperative skull images [15], to eliminate the remaining manual skull alignment step and complete the end-to-end automated pipeline. Force feedback for dura detection [6] represents a further, longer-term enhancement.

5. Conclusion

This paper has presented a modular, open-source stereotaxic automation system achieving beyond 0.1 mm positional accuracy [1] and 0.1 mm/min tissue-safe brain insertion speed [5] using commercially available open-source hardware and software. The nominal microstep increment is 0.0915 µm; experimentally, positional agreement was confirmed at 0.1 mm positioning accuracy. The central technical contribution is the domain adaptation of a 3D printing motion controller (Duet 3 Mini 5+) to neuroscience through open developer collaboration: a single firmware parameter (M203 I{0.1}) unlocks the ultra-low feed rate that enables controlled brain insertion, and a custom Ephys Link binding connects neuroanatomical atlas-based trajectory planning directly to hardware execution.

Building on the retrofit concept of Coffey et al. [7], the system adds safety-aware motion sequencing (Z retraction before lateral repositioning), mode-differentiated speeds (30 mm/min above the brain; 0.1 mm/min inside tissue), automated microinjection, and a purpose-built mechanical housing, delivering a complete, documented, end-to-end pipeline from pre-operative planning to needle insertion. The fully open and replicable design provides an accessible alternative to proprietary closed robotic systems [6].

To support adoption beyond the originating laboratory, a step-by-step replication guide for researchers with an existing stereotaxic frame who wish to implement the automation, and a surgical user manual covering end-to-end procedure execution via Pinpoint and Ephys Link is openly available at https://github.com/WinterLab-Berlin.

References

[1] De Vloo, P., & Nuttin, B. (2019). Stereotaxy in rat models: Current state of the art, proposals to improve targeting accuracy and reporting guideline. Behavioural Brain Research, 364, 457–463.

[2] Baker, M. (2016). 1,500 scientists lift the lid on reproducibility. Nature, 533(7604), 452–454.

[3] Voelkl, B., et al. (2020). Reproducibility of animal research in light of biological variation. Nature Reviews Neuroscience, 21, 384–393.

[4] Russell, W. M. S., & Burch, R. L. (1959). The Principles of Humane Experimental Technique. Methuen.

[5] Ferry, B., & Gervasoni, D. (2021). Improving stereotaxic neurosurgery techniques greatly reduces the number of rats used per experimental group. Animals, 11(9), 2662.

[6] Faria, C., et al. (2015). Review of robotic technology for stereotactic neurosurgery. IEEE Reviews in Biomedical Engineering, 8, 125–137.

[7] Coffey, K. R., Barker, D. J., Ma, S., & West, M. O. (2013). Building an open-source robotic stereotaxic instrument. Journal of Visualized Experiments, (80), e51006. doi:10.3791/51006

[8] Duet3D. (2024). Duet 3 Mini 5+ hardware and RepRapFirmware documentation. https://docs.duet3d.com

[9] Birman, D., et al. (2023). Pinpoint: Trajectory planning for multi-probe electrophysiology and injections in an interactive web-based 3D environment. eLife, 12, e91662.

[10] Virtual Brain Lab. Ephys Link: Middleware for connecting Pinpoint to external manipulators. https://ephys-link.virtualbrainlab.org

[11] Ly, P. T., et al. (2021). Robotic stereotaxic system based on 3D skull reconstruction to improve surgical accuracy and speed. Journal of Neuroscience Methods, 347, 108955.

[12] Han, D., et al. (2025). Robot-assisted stereotactic microinjection method for precision cell transplantation in rat and canine models. Cell Transplantation.

[13] Button, K. S., et al. (2013). Power failure: Why small sample size undermines the reliability of neuroscience. Nature Reviews Neuroscience, 14(5), 365–376.

[14] Paxinos, G., & Franklin, K. B. J. (2019). The Mouse Brain in Stereotaxic Coordinates (5th ed.). Academic Press.

[15] Zhou, P., Liu, Z., Wu, H., Wang, Y., Lei, Y., & Abbaszadeh, S. (2020). Automatically detecting bregma and lambda points in rodent skull anatomy images. PLoS ONE, 15(12), e0244378.

JOIN US AT THE NEXT EI!

electronic IMAGING

Imaging across applications . . . Where industry and academia meet!

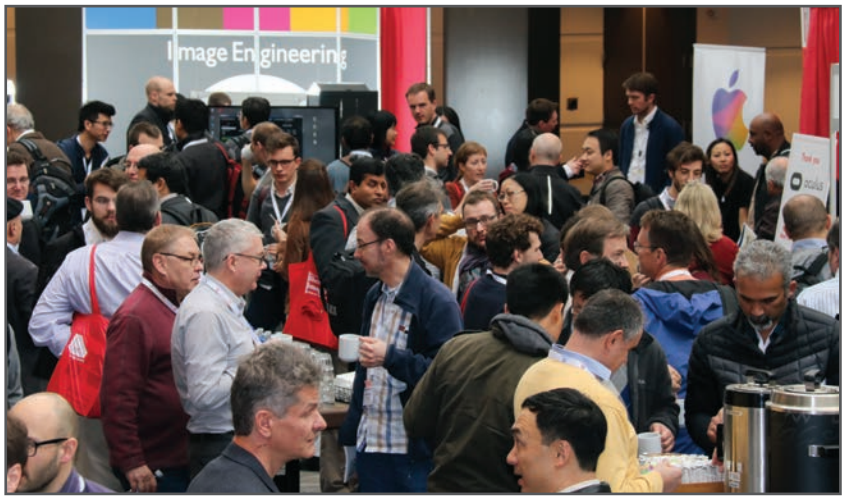

• SHORT COURSES • EXHIBITS • DEMONSTRATION SESSION • PLENARY TALKS •
• INTERACTIVE PAPER SESSION • SPECIAL EVENTS • TECHNICAL SESSIONS •

www.electronicimaging.org

ADVANCING IMAGING SCIENCE 75 1947 IS&T 2022 imaging.org